Polarization-resolved nonlinear dynamics in long-wavelength single-mode VCSELs subject to orthogonal optical injection

P. Pérez[1,2], A. Quirce[1,2], L. Pesquera[1], and A. Valle [1*].

[1]Instituto de Física de Cantabria, CSIC-Universidad de Cantabria, Avda. Los Castros s/n, E-39005, Santander, Spain.

[2] Departamento de Física Moderna, Universidad de Cantabria, Avda. Los Castros s/n, E-39005, Santander, Spain

ABSTRACT

In this work we perform an experimental study of the polarization-resolved nonlinear dynamics of a 1550 nm single-mode linearly polarized VCSEL when subject to orthogonal optical injection. We have measured the stability maps that identify the boundaries between regions of different nonlinear dynamics by using the RF-spectrum of the total power. These maps are measured in the plane of the frequency detuning between the injected light and the orthogonal linear polarization of the VCSEL versus injected power. Stability maps are obtained for two different values of the bias current. Analysis of the dynamics is given in terms of the time traces of the total power and of both linearly polarized output signals. The corresponding RF and optical spectra are also measured. Different dynamical regimes including periodic, period doubling, and irregular dynamics are observed for both polarizations. When the frequency detuning is positive polarization switching can be observed in a periodic dynamical regime, including both period one and period two behaviours. For positive frequency detuning, the only polarization that contributes to the dynamics of the total power is the orthogonal polarization. For negative frequency detuning values both linear polarizations contribute to the dynamics of the total power.

Keywords: Semiconductor lasers, vertical-cavity surface-emitting laser (VCSEL), polarization switching, injection locking, nonlinear dynamics.

1. INTRODUCTION

The performance of semiconductor lasers can be improved by injecting light emitted by another laser [1-3]. The optical injection technique can be used for reducing the laser linewidth, the mode partition noise or for enhancing the modulation bandwidth without modifying the semiconductor laser design. Interest in optical injection in vertical-cavity surface-emitting lasers (VCSELs) has recently increased [4-8] due to the inherent advantages of this type of semiconductor lasers. These include single-longitudinal mode operation, circular beam profile, reduced fabrication costs, ease of fabrication of 2D arrays, etc. [4]. Optical injection in semiconductor lasers is also interesting from the fundamental point of view because a wealth of complex nonlinear dynamics and bifurcations are obtained [9]. These include period doubling, quasiperiodicity, chaos, and injection locking [9]. These studies have been extended to VCSELs [10-35] since these devices offer additional degrees of freedom, like the direction of the emitted polarization and the presence of multiple transverse modes, when compared with their edge-emitting counterparts. The behaviour of these systems not only includes the previously mentioned dynamical regimes but also Polarization Switching (PS) and optical bistability.

Early experiments considered short wavelength devices in which the polarizations of both the VCSEL and the optical injection were parallel [10]. Nonlinear dynamics of VCSELs under orthogonally polarized optical injection has been experimentally and theoretically analyzed for 850 [11-23] and 1550-nm [24] wavelength devices. In this configuration linearly polarized light from an external laser is injected orthogonally to the linear polarization of a free-running VCSEL [25]. Additional studies on the long-wavelength devices used in telecommunications are of interest in present and future optical telecommunication networks.

*e-mail: valle@ifca.unican.es; phone 34 942 201465; fax: 34 942 200935

Most ot the studies on nonlinear dynamics of VCSELs subject to optical injection have been conducted with devices characterized by small values of the birefringence and showing PS in absence of optical injection. Rich nonlinear dynamics have been found including period doubling, quasi-periodicity, injection locking, bistability and chaos [13-23]. A mapping of the dynamics identifying boundaries between those behaviors was presented in [14]. Only recently the nonlinear dynamics of a 1550-nm wavelength single transverse mode VCSEL subject to orthogonal optical injection has been experimentally analyzed [24]. This device was characterized by very large values of the birefringence parameter and by emission in a single linear polarization over the whole bias current range in absence of optical injection. A stability map was obtained using the RF spectra of the total power to identify the boundaries between regions of different behavior. Periodic dynamics, PS and irregular and possibly chaotic behaviour were obtained [24]. However that work only reported the analysis of the dynamics of the total power because only measurements of their RF spectra and temporal traces were performed.

In this work we extend the experimental study of [24] by measuring the polarization-resolved nonlinear dynamics of a long-wavelength VCSEL when subject to orthogonal optical injection. Our VCSEL is the same device studied in [24]. Measured stability maps identifying the boundaries between regions of different nonlinear dynamics are reported for two different values of the bias current. We analyze the dynamics by measuring the time traces of the total power and of the power of both linear polarizations. RF and optical spectra of both linear polarizations and of the total power are also measured. A rich variety of nonlinear behaviours including periodic, period doubling, and irregular dynamics are observed for both polarizations and for the total power. More complex dynamics are observed as the bias current is increased. Analysis of the dynamics in terms of the frequency detuning between the injected light and the orthogonal linear polarization of the VCSEL is also performed. Our results show that the contribution of the linear polarizations to the dynamics of the total power depends on the sign of the frequency detuning.

Our paper is organized as follows. The experimental setup is described in Section II. Nonlinear dynamics for small and large values of the bias current are analyzed in sections III and IV, respectively. Finally, in section V, a summary and conclusions are presented.

II. EXPERIMENTAL SET-UP

We have used the all-fibre set-up shown in Fig. 1 to inject the light from a tunable laser into a quantum-well 1550 nm VCSEL. A commercially available VCSEL (Raycan™) is used in our experiments. Measurements of the dynamics of the total power emitted by this device were reported in [24]. The VCSEL bias current and temperature are controlled, respectively, by a laser driver and a temperature controller. The temperature is held constant at 298 ^{o}K during the experiments.
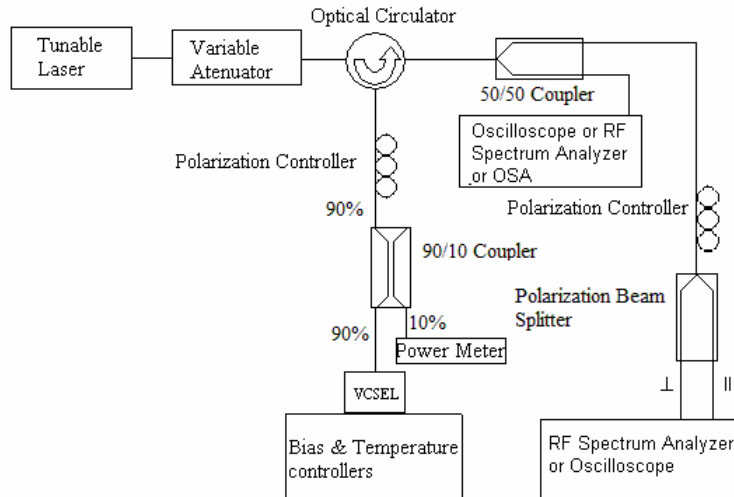
Fig. 1. Experimental set-up of orthogonal optical injection in a VCSEL.

A variable optical attenuator is included after the tunable laser to control the power of the optical injection. The output of the tunable laser is then injected into the VCSEL using a three-port optical circulator. Orthogonal optical injection is obtained by using a fibre polarization controller connected to the second port of the circulator. A 90/10 fibre directional coupler divides the optical path in two branches; the 10% branch is used to monitor the optical input power with a power meter whereas the 90% output is directly connected to the VCSEL. The reflected output of the VCSEL is analyzed by connecting different measurement equipment to the third port of the circulator. One half of the power is used to obtain the time traces of the total power at the oscilloscope with bandwidth of 6 GHz. The oscilloscope is substituted by a electrical spectrum analyzer for measuring the RF spectrum of the total power or by an Optical Spectrum Analyzer (OSA) for measuring the optical spectra. We have also used a Fabry-Perot (FP) analyzer to obtain optical spectra with a better resolution. The other half of the power is directed to a polarization beam splitter that selects the polarization direction in which the time traces or the RF spectra are measured. A high speed photodetector (9 GHz bandwidth) was connected before the oscilloscope or the RF analyzer for measuring the time traces and the RF spectra, respectively.

The L-I characteristics of the free-running VCSEL is shown in Fig. 2(a). The VCSEL emits in the fundamental transverse mode with a threshold current of I_{th}=1.64 mA. The VCSEL emits in a linear polarization which we will call the "parallel" polarization. Emission in the parallel polarized fundamental mode is obtained along the whole current range. Fig. 2(b) shows the optical spectrum of the VCSEL biased at 8 mA (4.88 I_{th}). The lasing mode of the device with parallel polarization is located at the wavelength $\lambda_{||}$ = 1536.6 nm. The subsidiary mode corresponds to the fundamental transverse mode with "orthogonal" polarization and its wavelength ($\lambda_{\perp}$) is shifted 0.49 nm to the long-wavelength side of the lasing mode. This value for the frequency splitting between the two orthogonal polarizations is very large in comparison to those reported in short-wavelength devices [14]. A Side Mode Suppression Ratio (SMSR) of 43 dB is measured for the orthogonal polarization. Spectra of this form are measured for all biases and no PS is observed for bias current above the threshold value. This is probably due to a large value of the dichroism parameter for our device.
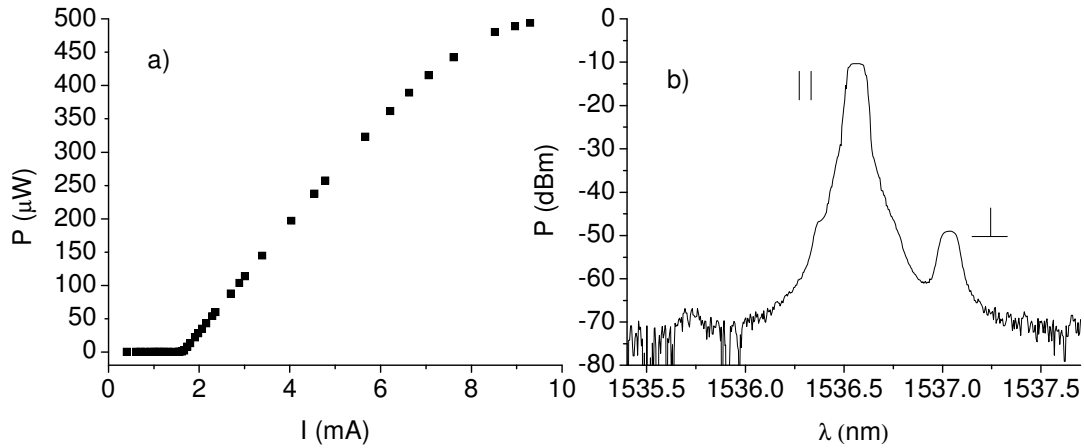
Fig. 2. (a) Light-current characteristics of the VCSEL without optical injection. (b) Optical spectrum of the free-running VCSEL (I_{VCSEL}=8 mA).

III. NONLINEAR DYNAMICS AT SMALL BIAS CURRENT

The dynamical behavior of our system can be summarized by using stability maps. We have used the RF spectra of the total power to distinguish between different dynamical regimes. The optical injection is characterized by its strength, given by the value of the optical power arriving at the VCSEL, P_{inj}, and by its frequency, ν_{inj}. We consider values of ν_{inj}, that are close to the frequency of the perpendicular polarization, $\nu_{\perp}$, the frequency detuning being $\Delta\nu = \nu_{inj} - \nu_{\perp}$. The experimental stability map is obtained by fixing a value of $\Delta\nu$ and increasing P_{inj} from low values. Different dynamical behaviours of the total power are plotted with different colours in the stability map of Fig. 3. Measurements are performed with the VCSEL biased with an applied current of 4 mA (2.44 I_{th}). The relaxation oscillation frequency of the free-running VCSEL, ν_R, is 2.95 GHz. In Fig. 3 the region P1 shows periodic (period 1) behaviour, region IR corresponds to irregular and possibly chaotic dynamics, and region SL represents the stable locking range.
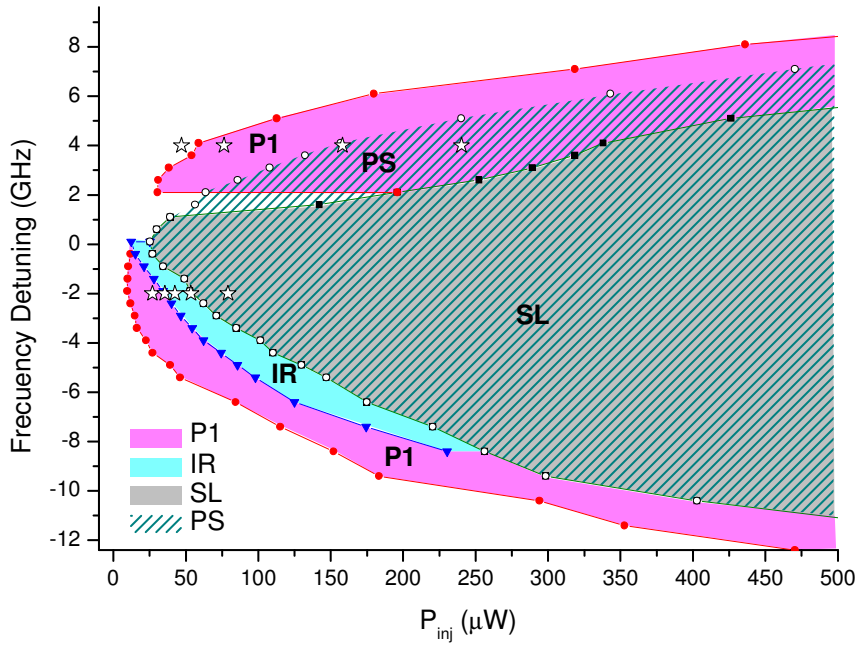
Fig. 3. Stability map of the VCSEL subject to orthogonal optical injection. Different regions are observed: SL (stable injection locking), P1 (period 1), IR (irregular dynamics), and PS (polarization switching). The stars mark the situations analyzed in Figs 4 and 5. Applied bias current of 4 mA.

We have considered P1 dynamics when the peak in the RF spectrum measured in the RF analyzer is 10 dB above the noise floor. The injected power required for PS to the orthogonal polarization of the VCSEL is also shown in Fig. 3. It is found that PS is always accompanied with stable locking for negative $\Delta \nu$. However, PS can be also observed in a periodic (P1) dynamical regime for positive values of $\Delta \nu$. RF spectra for the two polarizations and for the total power are shown in the left column of Fig. 4 for different dynamical regimes. They correspond to a fixed frequency detuning of 4 GHz and different values of P_{inj}. The cases considered in Fig. 4 are identified in Fig. 3 with white stars. The corresponding time traces of the total power and of the power of both linear polarizations are shown in the right column of Fig. 4. We note that the time traces have not been simultaneously recorded because only one high-speed photodetector was available in our experiment. A direct comparison between the powers of the time traces can not be done because of the different losses suffered by the total and polarization-resolved powers.

Fig. 4(a) shows the RF spectra just before reaching the P1 region. The RF spectra shown in this work have been obtained by subtracting the RF spectra in the absence of light to the RF spectra with optical injection. We have done it in order to subtract the noise in the photodetector and RF analyzer. A peak in the RF spectrum of the total power appears near the frequency detuning. A similar peak appears in the RF spectrum of the orthogonal polarization power. Oscillations of small amplitude around the steady state characterize both linear polarizations and the total power as it is shown in Fig. 4(b). The amplitude of the oscillations is smaller for the parallel polarization because its spectrum is flat as it is illustrated in Fig. 4(a). A clear P1 dynamics in the total and orthogonal polarized powers is obtained when increasing P_{inj} as it is shown in Figs. 4(c-d). Optical spectra obtained with the FP analyzer show that the orthogonal polarization of the VCSEL is excited. The frequency difference between the orthogonal polarization of the VCSEL and the injection frequency corresponds to the frequency of the peak in the RF spectrum. This is an indication of a periodic dynamics caused by beating between the optical injection and the orthogonal mode of the VCSEL. The parallel polarization keeps on being constant without contributing to the dynamics of the total power because its RF spectrum is weak and flat (see Fig. 4(c)). In Figs. 4(c-d) the VCSEL has not reached the PS region yet because the parallel polarization is still appreciable in the OSA spectrum. We have used the optical spectra obtained with the OSA to depict the PS region in Fig. 3. Our criterion has been the following: PS is achieved when the ratio between the power of the orthogonal and parallel polarizations is higher than 30 dB. The situation in which PS and P1 dynamics is obtained is illustrated in Figs. 4(e-f).

We note that the time traces of the parallel polarization in Figs. 4(f,h,j) is mainly due to the noise in the experimental set-up.The peaks appearing at the RF spectrum have shifted to larger frequency values. The frequencies of the times traces of the total and orthogonal polarized powers have increased to the values at which RF spectra have their peaks in Fig. 4(e). An increase of P_{inj} produces a larger amount of stimulated recombination of carriers and hence a smaller carrier density. In this way the refractive index and the wavelength of the orthogonal polarization increase producing a larger frequency detuning in the optical spectrum, that is a "frequency pushing" effect. We have observed this frequency pushing effect in our optical spectra. Peaks in the RF spectrum appear at larger frequencies because they appear at the value given by the frequency detuning in the optical spectrum obtained in the presence of optical injection.
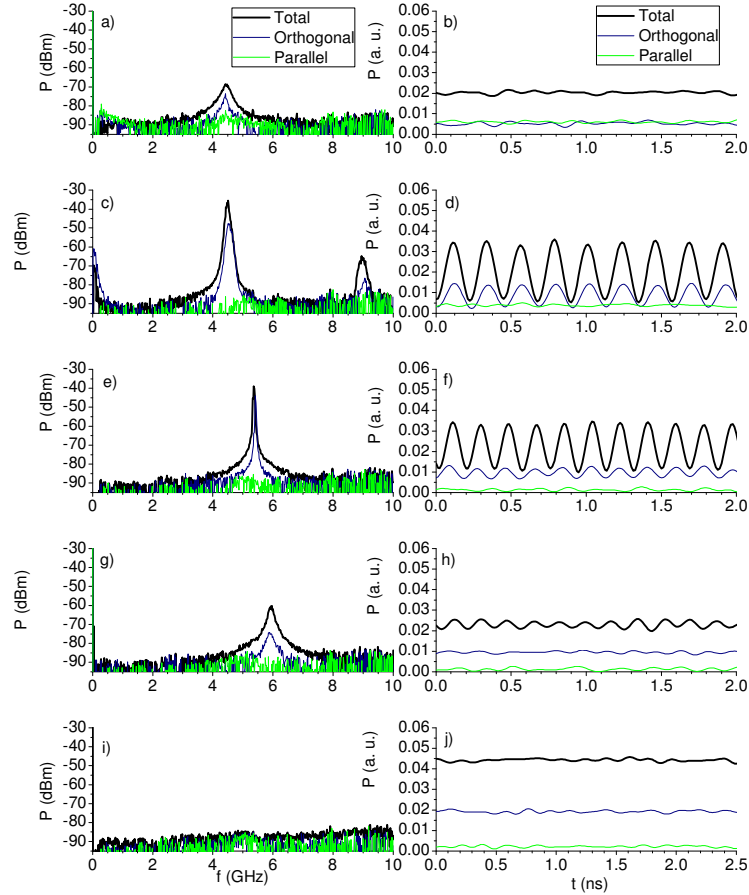
Fig. 4. (Left column) RF spectra of the total and polarized powers. (Right column) Time traces of the total power and of the power of both linear polarizations. Several values of injected power are considered: (a,b) P_{inj}= 47 µW, (c,d) P_{inj}= 76.4 µW, (e-f) P_{inj}=158 µW, (g,h) P_{inj}= 240.3 µW, and (i,j) P_{inj}= 1275.5 µW. The frequency detuning is $\Delta\nu$ = 4 GHz and the bias current is 4 mA.

Further increase of P_{inj} produces a decrease of the amplitude of the peaks in the RF spectrum (see Fig. 4(g)) and also of the amplitude of the oscillations of the time traces (see Fig. 4(h)). Operation in the SL regime is illustrated in Figs. 4(i-j). The RF spectra and the time traces of the total power and of the power of both linear polarizations become flat. The flatness of the RF spectrum is the criterion that we have used to depict the SL region in Fig. 3. We have also checked in the optical spectrum that the orthogonal polarization mode of the VCSEL is stably locked to the optical injection. We note that stable injection locking is observed for larger injected powers than those required for PS when $\Delta\nu$>0 . This is in contrast with results reported in [14] in which no locking of the fundamental mode was observed for $\Delta\nu$>0. This is an indication of the different role played by the much larger values of our birefringence parameter when compared to those considered in [14].

Fig. 5 shows the RF and time traces for a negative value of the frequency detuning, $\Delta\nu$= -2 GHz. The positions in the stability map of the cases analyzed in Fig. 5 are indicated in Fig. 3 with white stars. Figs. 5(a-b) illustrate the behavior obtained for small values of P_{inj}, in such a way that the system is in the P1 regime. RF spectra of both polarizations and total power have peaks at 1.9 GHz frequency and their harmonics. This frequency corresponds to the frequency detuning observed in our FP analyzer. Figs. 5(a-b) also shows that in contrast with Fig. 4 both polarization modes have periodic dynamics. The large amplitude of the harmonics in the RF spectrum is related to the non-sinusoidal shape of the time traces in contrast to those shown in Fig. 4. Periodic behavior in both polarizations was also obtained for 850-nm wavelength VCSELs [18]. Increasing P_{inj} produces an increase of the wavelength of the orthogonal polarization mode in such a way that the frequency detuning decreases. In this way the major peaks of the RF spectra of both polarizations and total power appear at a smaller value of the frequency, as it is shown in Fig. 5(c). Comparison between Figs. 5(b)-(d) shows that the frequency of the periodic time traces decreases as P_{inj} is increased.
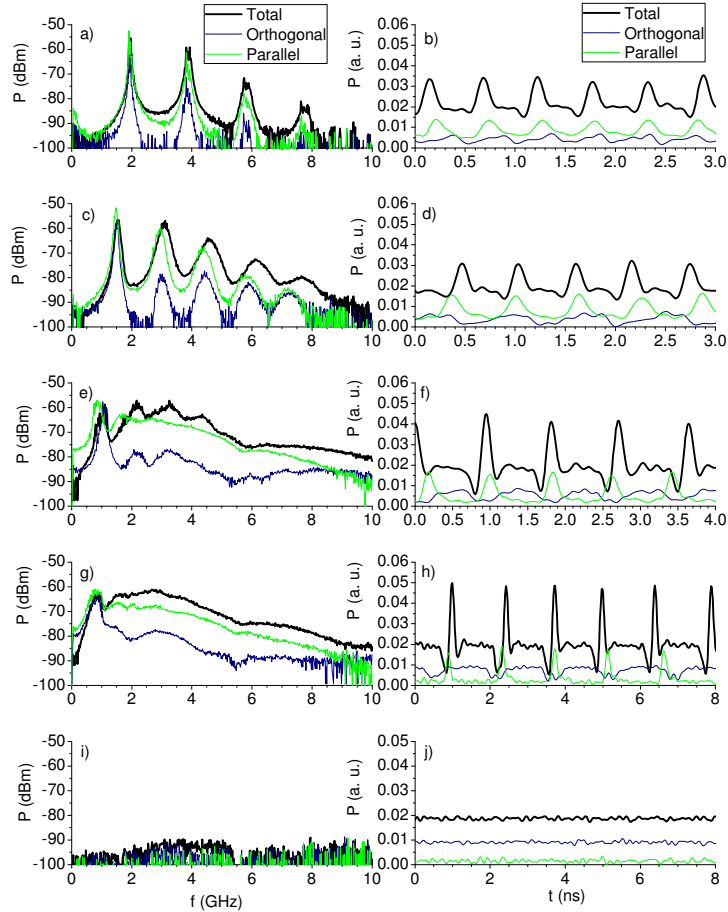
Fig. 5. (Left column) RF spectra of the total and polarized powers. (Right column) Time traces of the total power and of the power of both linear polarizations. Several values of injected power are considered: (a,b) P_{inj}= 26.9 μW, (c,d) P_{inj}= 35.5 μW, (e-f) P_{inj}=42.4 μW, (g,h) P_{inj}= 53.6 μW, and (i,j) P_{inj}= 79.1 μW. The frequency detuning is $\Delta\nu$ = -2 GHz and the applied bias current is 4 mA.

The peaks in the RF spectra tend to disappear as P_{inj} is increased as it can be seen in Fig. 5(e). Broad spectra are obtained that are the signature of irregular dynamics (IR region in Fig. 3). A better defined peak appears near 1 GHz frequency that approximately corresponds to the average value of the time between consecutive large amplitude peaks (interpulse time) in Fig. 5(f). Broadening of the RF spectra are caused by the dispersion of the interpulse time values. Fig. 5(e) shows that the RF spectra corresponding to the total and parallel polarized powers are much broader than that of the orthogonal polarized power. This corresponds to large (small) dispersion values of the interpulse time for the total and orthogonal (parallel) polarizations. Comparison between different time traces in Fig. 5(f) shows that the large amplitude

peak of the total power is due to the large amplitude peak of the parallel polarization. Also the plateau with small oscillations that appear in the total power after the large amplitude peak is basically due to the plateau observed in the orthogonal polarization. Figs. 5(g-h) show the spectra when P_{inj} is increased to 53.6 μW, such that the system is near the border between the IR and PS regions in Fig. 3. Peaks in the broad RF spectra are less defined than those in Fig. 5(e). Comparison between Figs. 5(f)-(h) shows that the interpulse time increases because the duration of the plateau of the total power is longer as P_{inj} increases (the averaged interpulse time corresponding to the total power is 0.87 and 1.83 ns for Fig. 5(f) and 5(h), respectively). This means that as the PS region is approached the VCSEL is orthogonally polarized with a constant power during a longer time. In fact PS is obtained by increasing slightly P_{inj} to 65 μW. The standard deviation of the interpulse time corresponding to the total power is 0.05 and 0.31 ns for Fig. 5(f) and 5(h), respectively. This explains the broader spectrum of the total power in Fig. 5(g) when compared to that of Fig. 5(e). We also note that Figs. 5(e,g) show that the RF spectra of the total power is much smaller at low frequencies than those corresponding to the polarization-resolved powers (polarization mode partition noise). This suggests some anticorrelation between the powers of both polarizations. Some indication of this anticorrelation can be seen in Figs. 5(f,h). Simultaneous measurement of both polarizations would be required to confirm the anticorrelated behavior. A sudden decrease of the RF spectra to the flat shape characteristic of SL is also obtained at that injected power value. Spectra and time traces corresponding to the SL regime are illustrated in Figs. 5(i-j) when P_{inj} = 79.1 μW.

IV. NONLINEAR DYNAMICS AT LARGE BIAS CURRENT

The stability map corresponding to a bias current value of 8 mA (4.88 I_{th}) is shown in Fig. 6. There are several differences with respect to the stability map discussed in the previous section. First, period doubling (P2) dynamics is obtained for positive and negative $\Delta\nu$ values. Second, PS can be observed in a periodic dynamical regime including P2 behavior. Third, the PS and the SL regions become more asymmetric as the current is increased, as it was obtained in [34] and [35], respectively. Although it is not shown in the Figure, SL is also observed for P_{inj}>1 mW for positive frequency detunings such that $\Delta\nu$ < 6GHz. As in Fig. 3, PS is always accompanied with SL for negative $\Delta\nu$. Also the irregular behavior is only obtained for negative values of $\Delta\nu$.
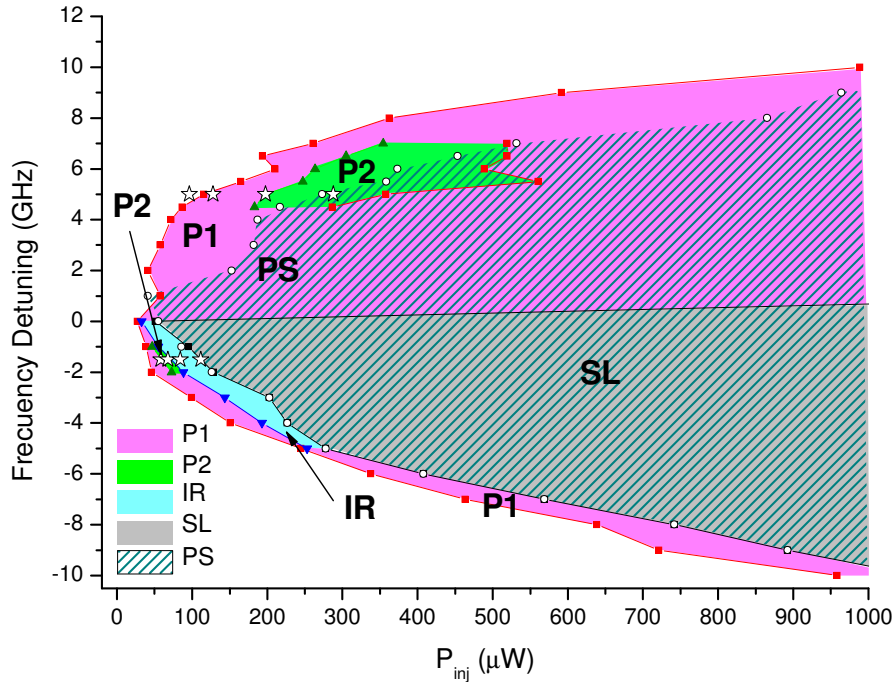
Fig. 6. Stability map of the VCSEL subject to orthogonal optical injection. Different regions are observed: SL (stable injection locking), P1 (period 1), P2 (period 2), IR (irregular dynamics), and PS (polarization switching). The stars mark the situations analyzed in Figs 7 and 8. Applied bias current of 8 mA.

RF spectra and time traces are shown in Fig. 7 for different dynamical regimes. They correspond to a fixed frequency detuning of 5 GHz and different values of P_{inj}. The cases considered in Fig. 7 are identified in Fig. 6 with white stars. Fig. 7(a) show the dynamics near the border of the P1 region. A peak in the RF spectra of the total power and of both linear polarizations appear near 5.5 GHz that is near the frequency difference between the peaks observed in the optical spectrum corresponding to the orthogonal polarization of the VCSEL and the injected frequency. A similar situation, with oscillations of larger amplitude, is obtained near the border but inside the P1 region as illustrated in Figs. 7(c-d). As we move further inside the P1 region the RF peak corresponding to the parallel polarization disappears while those corresponding to the orthogonal polarization and total power are maintained. Period doubling dynamics is obtained as it is shown in Fig. 7(e). Two well defined peaks appear near 3.1 and 6.2 GHz. These frequencies are near the relaxation oscillation frequency of the free-running VCSEL, ν_R, and $2\nu_R$ (ν_R measured at 8mA is 3.5 GHz). This is probably due to a subharmonic resonance. In the situation illustrated in Figs. 7(e-f) the polarization of the VCSEL has not switched yet, as it can be seen in Fig. 6. Measurement of the optical spectrum with the OSA shows that the parallel polarization is still excited and its flat and very weak RF spectrum indicates that it does not contribute to the dynamics of the total power because (see Fig. 7(e)).
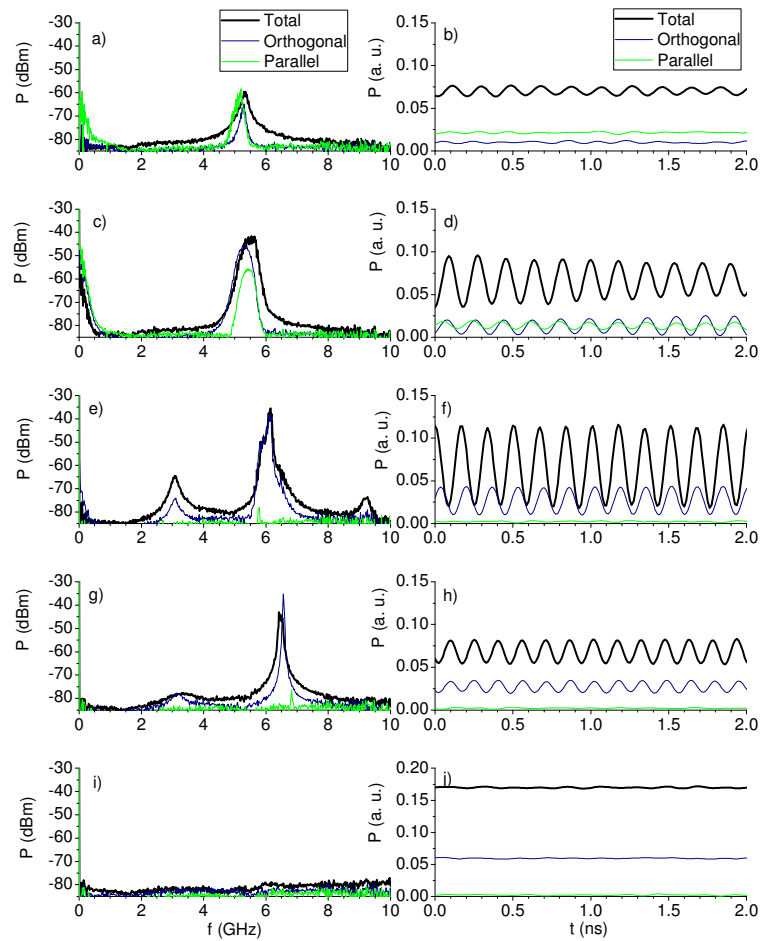
Fig. 7. (Left column) RF spectra of the total and polarized powers. (Right column) Time traces of the total power and of the power of both linear polarizations. Several values of injected power are considered: (a,b) P_{inj}= 96.1 µW, (c,d) P_{inj}= 127.6 µW, (e-f) P_{inj}=197.3 µW, (g,h) P_{inj}= 287.8 µW, and (i,j) P_{inj}= 3301.8 µW. The frequency detuning is $\Delta\nu$= 5 GHz and the applied bias current is 8 mA.

Fig. 7(g) illustrates the spectra when PS has been achieved. Both, the orthogonal polarization and the total power have P2 dynamics as it can be seen in Fig. 7(g). PS is then observed in a periodic dynamical regime including P2 behavior.

Further increase of P_{inj} produces P1 and SL (see Figs. 7(i-j)) dynamics.

Fig. 8 shows RF spectra and time traces for a negative $\Delta\nu$ value of -1.5 GHz. White stars in Fig. 6 show the position in the mapping of the cases analyzed in Fig. 8. Figs. 8(a-b) illustrate the P1 dynamics obtained at low values of P_{inj}. RF spectra of both polarizations have peaks at 3 GHz frequency and their harmonics. P2 dynamics is obtained for both linear polarizations when increasing P_{inj} as it can be seen in Fig. 8(c). Fig. 6 shows that the region in which P2 dynamics appears is very narrow. Figs. 8(a),(c) show that in contrast with the results obtained at positive $\Delta\nu$ both polarization modes have periodic dynamics. Irregular dynamics in both linear polarizations is obtained in Figs. 8(e)-(f). Dynamics is more irregular than those observed in Fig. 5(g-h). Peaks in the RF spectra are much more smeared, specially those corresponding to the RF spectrum of the orthogonal polarization. Also the time traces are more irregular than in Fig. 5(h). For instance two large amplitude consecutive peaks are occasionally obtained in the total power. This situation was not obtained in Fig. 5(h). Finally, Figs. 8(g-h) illustrate the dynamics when simultaneous SL and PS are achieved, just at the border between the IR and SL regions.
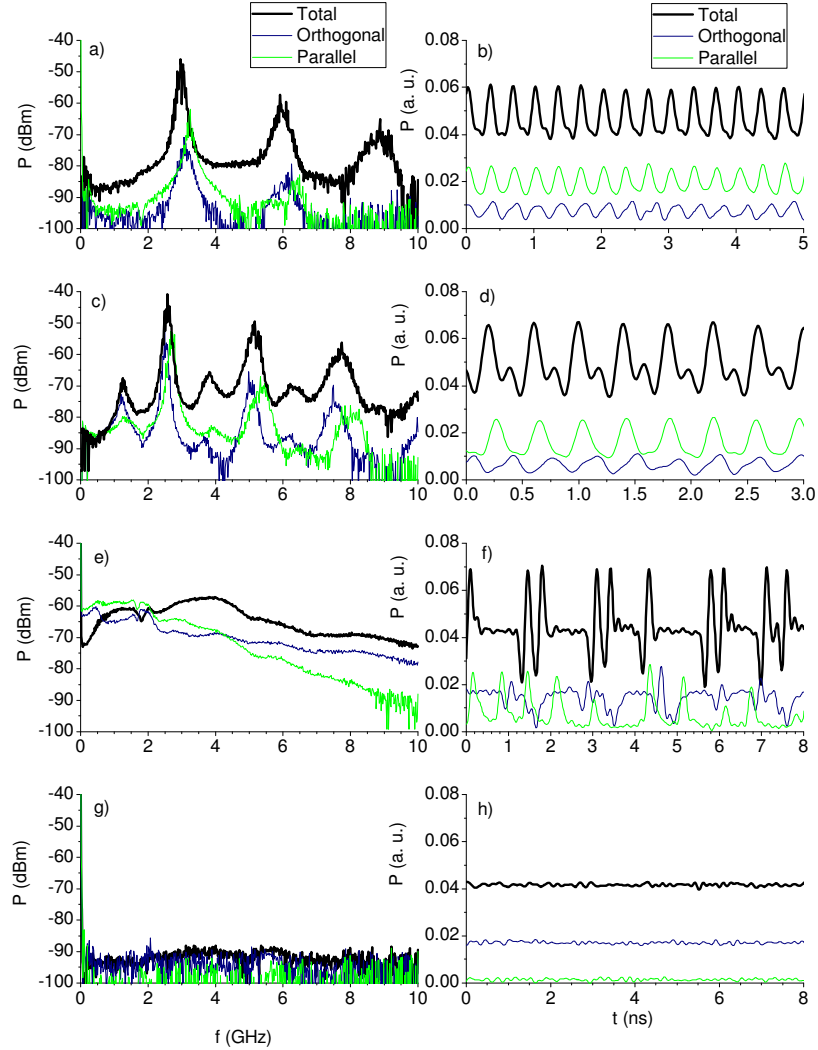
Fig. 8. (Left column) RF spectra of the total and polarized powers. (Right column) Time traces of the total power and of the power of both linear polarizations. Several values of injected power are considered: (a,b) P_{inj}= 58.5 µW, (c,d) P_{inj}= 67.6 µW, (e-f) P_{inj}=84 µW, and (g,h) P_{inj}= 111.2 µW. The frequency detuning is $\Delta\nu$ = -1.5 GHz and the applied bias current is 8 mA.

V. SUMMARY AND CONCLUSIONS.

In this work we have measured the polarization-resolved nonlinear dynamics of a 1550 nm single-mode VCSEL subject to orthogonal optical injection. These results have complemented our previous analysis of that system based just on the emitted total power [24]. Our VCSEL is characterized by emission in a single linear polarization over the whole bias current range in absence of optical injection and by very large values of the birefringence parameter. Stability maps identifying the boundaries between regions of different dynamics have been obtained for two different values of the bias current: 2.44 and 4.88 I_{th} times the threshold value. A rich variety of nonlinear behaviours including periodic, period doubling, and irregular dynamics have been observed for both linear polarizations. We have used time traces and RF spectra of the total and polarized powers to illustrate those dynamics. The dynamics becomes more complex as the bias current is increased. Injection locking and PS behaviours have been also analyzed as a function of the frequency detuning, $\Delta\nu$, between the injected light and the orthogonal linear polarization of the VCSEL. Injection locking has been obtained for larger (similar) injected powers than those corresponding to PS when $\Delta\nu>0$ ($\Delta\nu<0$). For positive values of $\Delta\nu$, PS can be observed in a periodic dynamical regime, including both period one and period two behaviors. Period two dynamics has been only observed for large values of the bias current, for both positive and negative $\Delta\nu$. We have shown that one of the main differences between results for positive and negative $\Delta\nu$ is the following. For $\Delta\nu>0$, the dynamics of the total power is determined by the dynamics of the orthogonal polarization as the injected power is increased. In this case the orthogonal polarization have periodic dynamics while the parallel polarization is characterized by a flat and much weaker RF spectrum. For $\Delta\nu<0$ both linear polarizations contribute to the dynamics of the total power. Situations have been described in which the parallel polarization has an irregular dynamics while the orthogonal polarization has irregular or periodic dynamics. In other situations both linear polarizations have periodic dynamics. Irregular dynamics has only been observed for negative values of the frequency detuning. Finally, simultaneous measurements of the time traces of the power of both linear polarizations will be done in future work to distinguish their contribution to the dynamics of the total power.

REFERENCES

[1] R. Lang, "Injection locking properties of a semiconductor laser", *IEEE J. Quantum Electron.* 18, no. 6, pp. 976-983, 1982.

[2] G. H. M. van Tartwijk, D. Lenstra, "Semiconductor lasers with optical injection and feedback", *Quantum Semiclass. Opt.* 7, pp. 87-143, 1995.

[3] M. J. Adams, A. Hurtado, D. Labukhin, and I. D. Henning, "Nonlinear semiconductor lasers and amplifiers for all-optical information processing", *Chaos*, vol. 20, art. 037102, 2010.

[4] F. Koyama, "Recent advances of VCSEL Photonics," *J. Lightwave Technol.* vol. 24, no. 12, pp. 4502-4513, Dec. 2006.

[5] C. H. Chang, L. Chrostowski, C. J. Chang-Hasnain, "Injection locking of VCSELs," *IEEE J. Select. Topics Quantum Electron.*, vol. 9, no. 5, pp.1386-1393, Sep./Oct 2003.

[6] D. Parekh, X. Zhao, W. Hofmann, M. C. Amann, L. A. Zenteno and C. J. Chang-Hasnain, "Greatly enhanced modulation response of injection-locked multimode VCSELs," *Opt. Exp.,* vol. 16, no. 26, pp. 21582-21586, Dec. 2008.

[7] D. Parekh, B. Zhang, X. Zhao, Y. Yue, W. Hofmann, M.C. Amann, A. Willner, and C. J. Chang-Hasnain, "Long distance single-mode fiber transmission of multimode VCSELs by injection locking", *Opt. Exp.*, vol. 18, no.20, pp. 20552-20557, 2010.

[8] T. Katayama, T. Ooi, and H. Kawaguchi, "Experimental demonstration of multi-bit optical buffer memory using 1.55-µm polarization bistable vertical-cavity surface-emitting lasers", *IEEE J. Quantum Electron.*, vol. 45, no. 11, pp. 1495-1504, Nov. 2009.

[9] S. Wieczorek, B. Krauskopf, T.B. Simpson and D. Lenstra, "The dynamical complexity of optically injected semiconductor lasers." *Phys. Rep.*, vol. 416, no. 1-2, pp. 1-128, Sep. 2005.

[10] H. Li, T. Lucas, J. G. McInerney, M. Wright, and R. A. Morgan, "Injection locking dynamics of vertical cavity semiconductor lasers under conventional and phase conjugate injection. "*IEEE J. Quantum Electronics*, vol. 32, no. 3, pp. 227-235, Feb. 1996.

[11] Y. Hong, K.A. Shore, A. Larsson, M. Ghisoni, and J. Halonen, "Pure frequency-polarisation bistability in vertical-cavity surface-emitting lasers subject to optical injection", *Electron. Lett.* 36, no. 24, pp. 2019-2020, 2000.

[12] Y. Hong, P.S. Spencer, P. Rees and K.A. Shore, "Optical injection dynamics of two-mode vertical cavity surface-emitting semiconductor lasers", *IEEE J. Quantum Electronics*, vol. 38, no. 3, pp. 274-278, Mar. 2002.

[13] Y. Hong, P. S. Spencer, S. Bandyopadhyay, P. Rees, and K. A. Shore, "Polarization resolved chaos and instabilities in a VCSEL subject to optical injection", *Opt. Comm.*, vol. 216, pp. 185-187, 2003.

[14] J. Buesa, I. Gatare, K. Panajotov, H. Thienpont, and M. Sciamanna, "Mapping of the dynamics induced by orthogonal optical injection in vertical-cavity surface-emitting lasers", *IEEE J. Quantum Electron.*, vol. 42, no. 2, pp. 198-207, Feb. 2006.

[15] I. Gatare, J. Buesa, H. Thienpont, K. Panajotov, M. Sciamanna, "Polarization switching bistability and dynamics in vertical-cavity surface-emitting lasers under orthogonal optical injection", *Optical and Quantum Electronics*. 38, pp. 429-443, 2006.

[16] I. Gatare, K. Panajotov, M. Sciamanna, "Frequency-induced polarization bistability in vertical-cavity surface-emitting lasers with orthogonal optical injection", *Phys Rev. A.* 75, 023804, 2007.

[17] M. Sciamanna and K. Panajotov, "Route to polarization switching induced by optical-injection in vertical-cavity surface-emitting lasers", *Phys. Rev. A*, vol. 73, no. 2, 023811, Feb. 2006.

[18] I. Gatare, M. Sciamanna, M. Nizette, and K. Panajotov, "Bifurcation to polarization switching and locking in vertical-cavity surface-emitting lasers with optical injection", *Phys. Rev. A*, vol. 76, no. 031803(R), 2007.

[19] A. Valle, I. Gatare, K. Panajotov, and M. Sciamanna, "Transverse mode switching and locking in vertical-cavity surface-emitting lasers subject to orthogonal optical injection", *IEEE J. Quantum Electron.* vol.43, pp.322-333, Apr. 2007.

[20] K. Panajotov, I. Gatare, A. Valle, H. Thienpont and M. Sciamanna, "Polarization- and Transverse-Mode Dynamics in Optically Injected and Gain-Switched Vertical-Cavity Surface-Emitting Lasers", *IEEE J. Quantum Electron.* vol.45, no.11, pp.1473-1481, Nov. 2009.

[21] I. Gatare, M. Sciamanna, M. Nizette, H. Thienpont and K. Panajotov, "Mapping of two-polarization-mode dynamics in vertical-cavity surface-emitting lasers with optical injection," *Phys. Rev. E.*, vol. 80, no. 026218, Aug. 2009.

[22] M. Nizette, M. Sciamanna, I. Gatare, H. Thienpont, and K. Panajotov, "Dynamics of vertical-cavity surface-emitting lasers with optical injection: a two-mode model approach", *J. Opt. Soc. Am. B*, vol. 26, no. 8, pp. 1603-1613, Aug. 2009.

[23] D. L. Boiko, G. M. Stéphan, and P. Besnard, "Fast polarization switching with memory effect in a vertical cavity surface emitting laser subject to modulated optical injection," *J. Appl. Phys.* 86, pp. 4096–4099, Oct. 1999.

[24] A. Hurtado, A. Quirce, A. Valle, L. Pesquera, and M. J. Adams, "Nonlinear dynamics induced by parallel and orthogonal optical injection in 1550 nm vertical-cavity surface-emitting lasers (VCSELs)", *Opt. Exp.*, vol. 18, no. 9, pp. 9423-9428, 2010.

[25] Z. G. Pan, S. Jiang, M. Dagenais, R. A. Morgan, K. Kojima, M. T. Asom, and R. E. Leibenguth, "Optical injection induced polarization bistability in vertical-cavity surface-emitting lasers," *Appl. Phys. Lett.*, vol. 63, no. 22, pp. 2999-3001, Nov.1993.

[26] K. H. Jeong, K. H. Kim, S. H. Lee, M. H. Lee, B. S. Yoo and K. A. Shore, "Optical injection-induced polarization switching dynamics in 1.5 µm wavelength single-mode vertical-cavity surface-emitting lasers," *IEEE Photon. Technol. Lett.,* vol. 20, no. 9-12, pp. 779-781, May. 2008.

[27] A. Hurtado, I. D. Henning, and M. J. Adams, "Two-wavelength switching with a 1550 nm VCSEL under single orthogonal optical injection," *IEEE J. Sel. Top. in Quantum Electron*, vol. 14, no. 3, pp. 911-917, May/Jun.2008.

[28] A. Valle, M. Gomez-Molina, and L. Pesquera, "Polarization bistability in 1550 nm wavelength single-mode vertical-cavity surface-emitting lasers subject to orthogonal optical injection," *IEEE J. Sel. Top in Quantum Electron.*, vol. 14, no. 3, pp. 895-902, May/Jun.2008.

[29] A. Hurtado, I. D. Henning, and M. J. Adams, "Different forms of wavelength polarization switching and bistability in a 1.55 μm vertical cavity surface-emitting laser under orthogonally polarized optical injection", *Opt. Lett*. 34, 365-367, 2009.

[30] A. Hurtado, D. Labukhin, I. D. Henning, and M. J. Adams, "Injection locking bandwidth in 1550-nm VCSELs subject to parallel and orthogonal optical injection", *IEEE J. Selec. Topics Quantum Electron*. 15, no. 3, pp. 585-593 2009.

[31] A. Quirce, A. Valle, and L. Pesquera, "Very wide hysteresis cycles in 1550 nm-VCSELs subject to orthogonal optical injection", *IEEE Phot. Tech. Lett*. 21, no. 17, pp. 1193-1195, 2009.

[32] A. Hurtado, A. Quirce, A. Valle, L. Pesquera, and M. J. Adams, "Power and wavelength polarization bistability with very wide hysteresis cycles in a 1550nm-VCSEL subject to orthogonal optical injection", *Opt. Exp*. 17, no. 26, pp. 23637-23642, 2009.

[33] M. S. Torre, A. Quirce, A. Valle, and L. Pesquera, "Wavelength-induced polarization bistability in 1550 nm VCSELs subject to orthogonal optical injection", *J. Opt. Soc. Am. B*, vol. 27, no. 12, pp. 2542-2548, 2010.

[34] M. S. Torre, A. Hurtado, A. Quirce, A. Valle, L. Pesquera, and M. J. Adams, "Polarization switching in long-wavelength VCSELs subject to orthogonal optical injection", *IEEE J. Quantum Electron.* To appear.

[35] N. Khan, K. Schires, A. Hurtado, I. D. Henning, and M. J. Adams, "Current dependence of polarization switching and locking in an optically injected 1550 nm VCSEL", *IET Optoelectronics*. To appear.